INFLUENCE OF ELECTRON AND NUCLEAR SPIN ON PHOTOFRAGMENT ALIGNMENT: APPLICATION TO ClCN DISSOCIATION AT 157.6 nm

J.A. GUEST, M.A. O'HALLORAN and R.N. ZARE*
Department of Chemistry, Stanford University Stanford California 94305, USA

Received 22 September 1983

The alignment determined from rotationally resolved CN emission following ClCN photodissociation does not describe the quadrupole moment of the nuclear rotation vector N' unless corrected for the depolarizing effects of nuclear and electron spin in the photofragment. When these adjustments are made, the anisotropy of the N' distribution in CN $B\,^2\Sigma^+$ indicates that the ClCN dissociation process at 157 6 nm proceeds via a direct mechanism that is independent of rotation.

1. Introduction

Triatomic molecules generally fragment when they are excited with photons of energy higher than their dissociation limit and lower than their ionization potential [1]. Often the photodissociation proceeds on a time scale so short that the triatomic absorption spectrum appears broad and nearly featureless. In such cases the absorption spectrum yields little information toward the elucidation of the potential surfaces in the excited parent species and the forces resulting in fragmentation. Attention has then turned to the study of the final-state distribution of the fragments with the goal of understanding the dissociation process [2–4].

Recently, there have been advances in interpreting photofragment fluorescence polarization in terms of the quadrupole alignment of the rotational angular momentum vector [5,6]. The alignment describes the nature of the spatial distribution of rotational angular momentum vectors N' by measuring the relative populations of small $|M'|$ states compared to large $|M'|$ states. This can be associated in turn with the state symmetry of the excited parent molecule and dynamics of the fragmentation by relation to the angular momentum transfer quantum number j_t, which characterizes separable photofragmentation amplitudes.

At low values of N', the observed alignment needs to be adjusted for the effects of spin angular momenta that are not aligned in the dipole process. This has been stressed in the interpretation of atomic fluorescence by Fano and Macek [7] Here we consider the molecular analog, in which unresolved spin–rotation and hyperfine structure are considered, in order to extract the alignment of the nuclear rotation of the molecule. We examine the photodissociation of cyanogen chloride at 157.6 nm

$$ClCN + h\nu \rightarrow Cl + CN\ B\,^2\Sigma^+$$

and illustrate these corrections on the measured alignment of the resulting dispersed CN $B\,^2\Sigma^+ – X\,^2\Sigma^+$ emission. The ClCN absorption band studied here has been assigned as a $\pi–\pi^*$ intravalence transition where the excited state is probably composed of bent components of $^1\Sigma^-$ and $^1\Delta$ states [8]. The treatment of the CN rotational alignment permits a characterization of the fragment anisotropy at low values of N', where it may be expected that particularly interesting relationships to the dissociation mechanism might occur [9,10].

2. CN B–X fluorescence polarization from ClCN

Cyanogen chloride was obtained from Matheson at >97% purity and degassed at liquid-nitrogen temperatures before use. The 157.5 and 157.6 nm output of an F_2 excimer laser (Lumonics TE 861) was used to photodissociate low pressure (25–40 mTorr) flowing

* Holder of a Shell Distinguished Chair, funded by the Shell Companies Foundation, Inc.

ClCN samples. The photolysis light, which ranged from 5 to 20 mJ/pulse, passed through a N_2 purge region and was mildly focused by a 30 cm lens to 18 cm before the fluorescence collection region. Photofragment fluorescence emission was collected at right angles to the laser propagation direction through a lens with a half angle of 9° and dispersed through a Spex 3/4 m monochromator. Dispersed emission intensities were normalized for incident light fluctuations using a photomultiplier and interference filter attached to the cell to monitor total CN B–X fluorescence.

For polarization measurements a commercial photoelastic modulator (Hinds PEM CF-4) and sheet polarizer were placed before the monochromator. The observed fluorescence polarization, P_{obs}, is defined by $P_{obs} = (I_{\parallel} - I_{\perp})/(I_{\parallel} + I_{\perp})$, where $I_{\parallel}$ and $I_{\perp}$ are the fluorescence intensities with electric vectors parallel and perpendicular to the laser propagation direction, respectively. The intensities $I_{\parallel}$ and $I_{\perp}$ were measured using the precise non-mechanical method of McClelland [11], in which the fluorescence is temporally synchronized with selected phases of the photoelastic modulator crystal oscillation. This technique has the advantage that the light passing into the monochromator always has the same plane of polarization, eliminating the need for a scrambler. A MgF_2 Rochon polarizer was used to analyze the linear polarization of the incident laser. The polarization was determined to be $-2 \pm 3\%$ relative to the vertical axis of the experiment. The incident laser light is thus effectively unpolarized, and P_{obs} is converted to the polarization P for linearly polarized light by the relation $P = 2P_{obs}/(1 + P_{obs})$.

Fig. 1a presents the fluorescence polarization at 0.03 nm resolution of selected rotational transition of the CN $B\,^2\Sigma^+ – X\,^2\Sigma^+$ (0–0) band following the photodissociation of 4×10^{-2} Torr of ClCN. Directly below the polarization measurements, fig. 1b shows the normalized CN B–X emission spectrum at the same resolution, recorded with a polarizer set at the magic angle (54.7°) with respect to the laser propagation axis to remove any dependence of the relative emission intensity on the photofragment alignement. The emission spectrum is independent of pressure from 7×10^{-3} to 3×10^{-1} Torr. The polarizations of selected transitions also remain unchanged when the ClCN pressure is increased up to 0.1 Torr.

The measured photofragment polarization is converted to the observed quadrupole alignment $\mathcal{A}_0^{(2)}(N'$, obs) by the relation [5–7]

$$\mathcal{A}_0^{(2)}(N', \text{obs}) = \frac{1}{h^{(2)}(N', N'')} \frac{4P}{3 - P}. \quad (1)$$

The geometrical factor $h^{(2)}(N', N'')$ accounts for the effect of the final state N'' on the fluorescence polarization of the $N' \rightarrow N''$ transition. The values for the product $h^{(2)}(N', N'')\,\mathcal{A}_0^{(2)}(N'$, obs) for the CN B–X emission are also shown in fig. 1a. The observed alignments of CN $B\,^2\Sigma^+$ for some low values of N' are listed in table 1. Data for N' greater than 8 are not analyzed because the P-branch lines become progressively less well resolved and the R-branch lines are overlapped by emission from $v' = 1$.

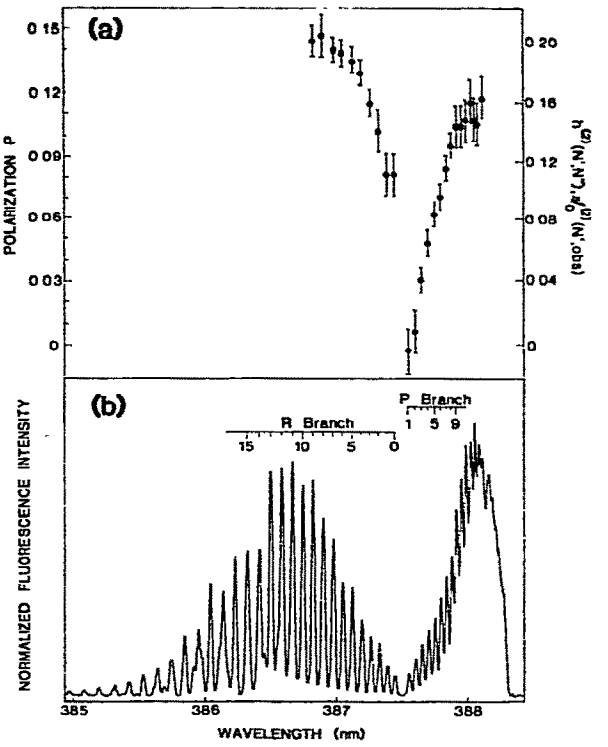

Fig. 1. (a) CN($B\,^2\Sigma^+ – X\,^2\Sigma^+$) photofragment fluorescence polarization measured for different rotational transitions in the (0,0) band at 0.03 nm resolution. (b) The normalized CN B–X photofragment emission spectrum following ClCN dissociation at 157.6 nm.

Table 1
Depolarization factors and alignments for CN B $^2\Sigma^+(v'=0)$

N'	$\bar{g}^{(2)}(N')$ [a]	$\bar{g}^{(2)}(N')$ [b]	P branch		R branch	
			$\mathcal{A}_0^{(2)}(N', \text{obs})$	$\mathcal{A}_0^{(2)}(N')$ [a]	$\mathcal{A}_0^{(2)}(N', \text{obs})$	$\mathcal{A}_0^{(2)}(N')$ [a]
1	0.098	0.276	−0 04 (0.07)	−0 44 (0.68)	−0.06 (0.01)	−0.57 (0 07)
2	0.374	0.437	−0 14 (0.03)	−0.37 (0.07)	−0 11 (0.01)	−0.30 (0.03)
3	0.615	0 633	−0.19 (0.02)	−0.31 (0.04)	−0.18 (0 02)	−0 28 (0.03)
4	0.751	0.758	−0.23 (0 02)	−0 31 (0.03)	−0.22 (0 01)	−0.30 (0.03)
5	0.828	0 831	−0.25 (0.02)	−0.30 (0.02)	−0.27 (0 01)	−0.32 (0.02)
6	0.875	0 877	−0.29 (0.02)	−0 33 (0.02)	−0.30 (0.01)	−0 34 (0.02)
7	0.905	0.906	−0.32 (0.02)	−0.35 (0 02)	−0.31 (0.02)	−0.35 (0.02)
8	0.926	0.926	−0.30 (0 02)	−0.32 (0 02)	−0.33 (0 02)	−0.35 (0.02)

[a] Calculated for coupling case $b'_{\beta J}$. [b] Calculated for coupling case $b_{\beta S}$

3. Adjustment of observed alignment for the effect of isotropically distributed angular momenta

3.1. Theory

The rotational alignment of the vector N' is not completely described by eq. (1), since the nuclear and electron spin angular momenta of the fragment have not been included in the analysis. Neither the unpaired electron spin nor the nuclear spin can be aligned in an electric-dipole process and we assume that they are randomly oriented. These spins couple to N' to form the resultant F', about which N' precesses. The observed alignment of N', $\mathcal{A}_0^{(2)}(N', \text{obs}; t)$, thus oscillates in time, attaining its maximum absolute value immediately after the photodissociation process. If the molecular spin–rotation interaction is large compared to its hyperfine coupling, then the angular momenta are coupled according to Hund's case $b_{\beta J}$ [12], where S' couples first to N' to give J' which then couples to I' to give the resultant F'. Here the observed alignment at time t is related to the "true" rotational alignment $\mathcal{A}_0^{(2)}(N')$ by

$$\mathcal{A}_0^{(2)}(N', \text{obs}; t) = \mathcal{A}_0^{(2)}(N')\,\bar{g}^{(2)}(N', t), \tag{2}$$

where [7,13]

$$\bar{g}^{(2)}(N', t) = \sum_{\substack{J'_1 J'_2 \\ F'_1 F'_2}} \frac{(2F'_1+1)(2F'_2+1)(2J'_1+1)(2J'_2+1)}{(2S'+1)(2I'+1)} \times \begin{Bmatrix} J'_1 & J'_2 & 2 \\ N' & N' & S' \end{Bmatrix}^2 \begin{Bmatrix} F'_1 & F'_2 & 2 \\ J'_1 & J'_2 & I' \end{Bmatrix}^2 \times \cos[2\pi\nu(J'_1F'_1; J'_2F'_2)\,t]. \tag{3}$$

The frequency $\nu(J'_1F'_1; J'_2F'_2)$ corresponds to the splitting between the levels $(J'_1F'_1)$ and $(J'_2F'_2)$ for a given N'. For a time-unresolved experiment where these frequencies are large relative to $(2\pi\tau)^{-1}$ where τ is the radiative lifetime, then eqs. (2) and (3) reduce to the simpler expressions

$$\mathcal{A}_0^{(2)}(N', \text{obs}) = \mathcal{A}_0^{(2)}\,\bar{g}^{(2)}(N') \tag{4}$$

and

$$\bar{g}^{(2)}(N') = \sum_{J'F'} \frac{(2F'+1)^2\,(2J'+1)^2}{(2S'+1)(2I'+1)} \times \begin{Bmatrix} J' & J' & 2 \\ N' & N' & S' \end{Bmatrix}^2 \begin{Bmatrix} F' & F' & 2 \\ J' & J' & I' \end{Bmatrix}^2. \tag{5}$$

If the hyperfine interaction in a $^2\Sigma$ molecule is large compared to its spin–rotation splitting, then the angular momentum coupling is described by Hund's case

$b_{\beta S}$, where I' and S' couple to form the resultant G', which then couples to N' to give F'. As before for a time-unresolved experiment where the frequency splittings are large compared to $(2\pi\tau)^{-1}$, the cross terms of the type $(J_1'F_1') \neq (J_2'F_2')$ become vanishingly small, and

$$\bar{g}^{(2)}(N') = \left(\sum_{G'F'} (2F'+1)^2 \begin{Bmatrix} F' & F' & 2 \\ N' & N' & G' \end{Bmatrix}^2 \right) \times \left(\sum_{G'} (2G'+1) \right)^{-1}. \quad (6)$$

The proper analysis of alignment data for various photofragment species depends on the treatment for the effects of nuclear and electron spin depolarization described above. The magnitudes of the $\bar{g}^{(2)}(N')$ corrections for various possible spins are presented in fig. 2. Depolarization factors $\bar{g}^{(2)}(N')$ for a single spin S' are shown in fig. 2a, while fig. 2b plots $\bar{g}^{(2)}(N')$ for $S' = 1/2$ (a doublet state) with various values of I' coupled in case $b_{\beta J}$. Fig. 2 shows that $\bar{g}^{(2)}(N')$ rapidly approaches unity as N' increases but $\bar{g}^{(2)}(N')$ is much less than unity for small N' values. Moreover, the presence of nuclear spin causes further reduction in the magnitude of $\bar{g}^{(2)}(N')$ and cannot be ignored even if it is unresolved (which is usually the case).

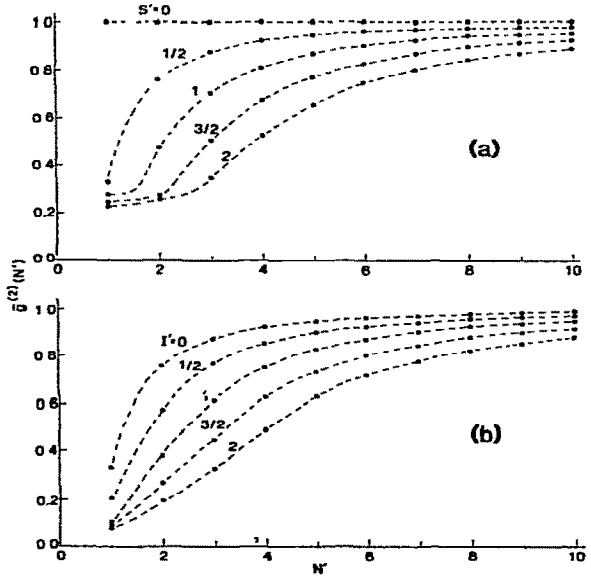

Fig. 2. (a) Depolarization factors $\bar{g}^{(2)}(N')$ for $S' = 0$, 1/2, 1, 3/2, and 2 as a function of N'. (b) Depolarization factors $\bar{g}^{(2)}(N')$ for a doublet state ($S' = 1/2$) coupled with $I' = 0$, 1/2, 1, 3/2, and 2 according to Hund's case $b_{\beta J}$.

3.2. Application to ClCN photodissociation

Since CN B $^2\Sigma^+$ has an unpaired electron spin $S' = 1/2$ and nuclear spin $I' = 1$, the depolarization adjustments outlined in section 3.1 are required to extract the rotational alignment of N' from the observed alignment. For CN in its B $^2\Sigma^+$ state, the $N \cdot S$ spin–rotation coupling constant γ' is 469.2 ± 1.2 MHz [14], and the $I \cdot S$ hyperfine coupling constant b' is 467 ± 10 MHz [15]. These interactions cause frequency splittings that are much larger than the natural linewidth, where the radiative lifetime is 65.6 ± 1.0 ns [16]. At high N', the spin–rotation interaction dominates and CN B $^2\Sigma^+$ is described well by Hund's coupling case $b_{\beta J}$. For low values of N', however, the large hyperfine interaction requires the angular momentum coupling in the CN B state to be characterized as intermediate between cases $b_{\beta J}$ and $b_{\beta S}$. In lieu of a full intermediate coupling treatment, it is instructive to calculate the depolarization factors $\bar{g}^{(2)}(N')$ for both cases separately using eqs. (5) and (6). They are included in table 1 for comparison. The time-unresolved depolarization factors are valid here even though the emission is measured for only 50 ns after each laser shot because the precessional period of N' about F' is much shorter.

Ambient magnetic fields in the experiment may cause additional fluorescence depolarization, according to the expression [13,17]

$$P = P_{\text{obs}}/[1 + 3.1 \times 10^{22}(Hg\tau)^2]. \quad (7)$$

Here H is the magnetic field in tesla perpendicular to the axis of cylindrical symmetry, g is the molecular electronic g factor, which varies as $\pm 1/(2N+1)$, P_{obs} is the observed polarization, and τ is the state lifetime. We find that the present polarized emission should not be significantly affected by the earth's 4×10^{-5} T field. Examination of eq. (7), however, shows that molecular states whose lifetimes are longer than 200 ns may exhibit significant fluorescence depolarization at low N'.

Fig. 3 compares the rotational alignments $\mathcal{A}_0^{(2)}(N')$ listed in table 1, to the limiting alignments for the allowed range of j_t. The value $j_t = N'$ corresponds to a Q branch in absorption and the average of $j_t = N' + 1$

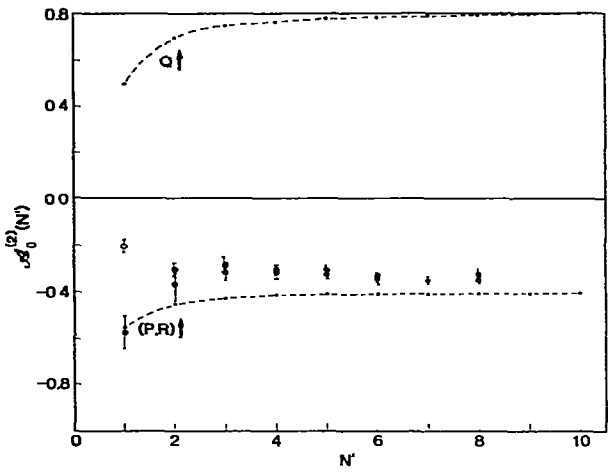

Fig 3. CN $B\,^2\Sigma^+(v'=0)$ rotational alignments determined in case $b_{\beta J}$ (closed circles with error bars) compared to limiting alignment values (dashed curve) The rotational alignment for $N'=1$ in case $b_{\beta S}$ is also shown (open circle).

and $j_t = N' - 1$ corresponds to a P,R branch in absorption [6]. The CN $B\,^2\Sigma^+$ rotational alignments are slightly smaller in magnitude than the $j_t = N' \pm 1$ limit at all N' except for $N'=1$. At $N'=1$ the rotational alignment will be intermediate to the two values shown in fig. 2 for the different coupling cases in the fragment. We find from these results that (1) the absorption dipole points essentially parallel to the ClCN internuclear axis, (2) the resulting CN $B\,^2\Sigma^+(v'=0)$ fragment has a rotational alignment *independent* of rotational state, and (3) the value of the alignment is approximately $-2/5$, which is the value expected [6,18] for this absorption/emission dipole moment geometry and direct fragmentation. The first conclusion is in accord with spectroscopic predictions [8]. Interpretation of the CN rotational and vibrational distribution in terms of the photodissociation mechanism will be presented in a future publication.

Acknowledgement

We thank Chris Greene for valuable discussions. This work was supported in part by the National Science Foundation under Grant No. NSF PHY 82-06400.

References

[1] H. Okabe, Photochemistry of small molecules, (Wiley–Interscience, New York, 1978)
[2] M.N R. Ashfold, M.T. Macpherson and J.P. Simons, in Topics in current chemistry, Vol 86 (Springer, Berlin, 1979) pp. 1–90.
[3] S.R. Leone, Advan. Chem. Phys 50 (1982) 255.
[4] M. Shapiro and R. Bersohn, Ann. Rev. Phys Chem 33 (1982) 409.
[5] C.H. Greene and R N Zare, Phys. Rev. A25 (1982) 2031
[6] C H Greene and R N Zare, Ann Rev. Phys. Chem. 33 (1982) 119
[7] U Fano and J.H Macek, Rev Mol Phys 45 (1973) 553.
[8] W.S Felps, S.P McGlynn and G L Findley, J. Mol Spectry. 86 (1981) 71.
[9] P Andresen and E.W. Rothe, J. Chem. Phys. 78 (1983) 989.
[10] J.P. Simons and A.J. Smith, Chem. Phys. Letters 97 (1983) 1.
[11] G.M. McClelland, Ph.D. Thesis, Harvard University, Cambridge, Massachusetts (1979)
[12] C.H. Townes and A.L. Schawlow, Microwave spectroscopy (Dover, New York, 1975).
[13] K. Blum, Density matrix theory and applications (Plenum Press, New York, 1981).
[14] T.J. Cook and D H. Levy, J. Chem. Phys 58 (1973) 3547
[15] K.M. Evenson, J L. Dunn and H P. Broida, Phys. Rev. 136 (1964) A1566,
H E. Radford, Phys Rev. 136 (1964) A1571.
[16] W M. Jackson, J Chem Phys. 61 (1974) 4177.
[17] A.C.G. Mitchell and M.W. Zemansky, Resonance radiation and excited atoms (Cambridge Univ. Press, London, 1961).
[18] M.T. Macpherson, J.P. Simons and R N Zare, Mol. Phys 38 (1979) 2049.